Published in final edited form as:

Mult Scler. 2018 November ; 24(13): 1687–1695. doi:10.1177/1352458517730132.

Cognitive Impairment and the Regional Distribution of Cerebellar Lesions in Multiple Sclerosis

SM Tobyne,
Neurology, Massachusetts General Hospital, Boston, MA, USA.

WB Ochoa,
Anatomy and Neurosciences, VU University Medical Center, Amsterdam, The Netherlands.

JD Bireley,
Neurology, Massachusetts General Hospital, Boston, MA, USA.

VMJ Smith,
Neurology, Massachusetts General Hospital, Boston, MA, USA.

JJ Geurts,
Anatomy and Neurosciences, VU University Medical Center, Amsterdam, The Netherlands.

JD Schmahmann,
Neurology, Massachusetts General Hospital, Boston, MA, USA.

EC Klawiter
Neurology, Massachusetts General Hospital, Boston, MA, USA.

Abstract

Background: Cerebellar lesions are often reported in relapsing remitting MS (RRMS), and have been associated with impaired motor function and cognitive status. However, prior research has primarily focused on summary measures of cerebellar involvement (e.g. total lesion load, gray/white matter volume) and not on the effect of lesion load within specific regions of cerebellar white matter.

Corresponding author: Eric C. Klawiter, 149 13th Street, Room 2503, Charlestown, MA 02129; eklawiter@nmr.mgh.harvad.edu; Phone: 617-726-7531; Fax: 617-726-6991.

Author Contributions

SMT, WBO, JDB, VMJS, and ECK designed and conceptualized the study. SMT, WBO, and ECK performed statistics analyses. SMT, JJG, JDS and ECK interpreted the data, drafted and revised the manuscript.

Potential Conflicts of Interest

Sean M. Tobyne reports no disclosures.

Wilson B. Ochoa reports no disclosures.

J. Daniel Bireley reports no disclosures.

Victoria M.J. Smith reports no disclosures.

Jeroen J.G. Geurts is (associate) editor of Multiple Sclerosis Journal and BMC Neurology; he has received consulting honoraria (and/or research support) from Biogen Idec, Novartis Pharma, and Sanofi-Genzyme.

Jeremy D. Schmahmann has received consulting fees from Ataxion, Biogen, Biohaven, Takeda and Pfizer.

Eric C. Klawiter has received research support from Atlas5d, Biogen Idec, EMD Serono, and Roche, and received consulting fees from Acorda Therapeutics, Atlas5d, Biogen Idec, EMD Serono, Genentech, and Shire.

Objective: Spatially map the probability of cerebellar white matter lesion occurrence in RRMS and explore the relationship between cognitive impairment and lesion (CWML) location within the cerebellum.

Methods: High resolution structural MRI was acquired on 16 cognitively impaired (CI) and 15 cognitively preserved (CP) RRMS subjects at 3T and used for lesion identification and voxel-lesion symptom analysis (VLSM).

Results: CI RRMS demonstrated a predilection for the middle cerebellar peduncle (MCP). VLSM results indicate that lesions of the MCP are significantly associated with CI in RRMS. Measures of cerebellar lesion load were correlated with age at disease onset but not disease duration.

Conclusion: A specific pattern of cerebellar lesions involving the MCP, rather than the total cerebellar white matter lesion load, contributes to cognitive dysfunction in RRMS. Cerebellar lesion profiles may provide a biomarker of current or evolving risk for cognitive status change in RRMS.

Keywords

Multiple sclerosis; cerebellum; cognitive dysfunction; Magnetic Resonance Imaging; Cerebellar White Matter

Introduction

While the role of the cerebellum in motor function has long been established, it is now also evident that that the cerebellum plays a major role in coordination of cognitive and affective processes.[1] Tract tracing studies in animals reveal precisely arranged anatomical pathways linking different cerebellar regions with sensorimotor, association and limbic areas of the cerebral hemispheres, and functional MRI investigations have identified task- and intrinsic connectivity network-specific topography in the cerebellum in patients and healthy controls.[1–4] These connections provide the critical underpinning of the cerebellar contribution to cognition, as shown for example, in functional MRI (fMRI) studies of executive function, language, attention and working memory.[5, 6] Damage to the cerebellum and/or its connections disrupts cerebrocerebellar circuitry, with cerebellar anterior lobe lesions causing the cerebellar motor syndrome, and cerebellar posterior lobe lesions producing the cerebellar cognitive affective syndrome[7, 8] characterized by deficits in executive function, visuospatial cognition, linguistic processing and emotional regulation.

MS results in cognitive impairment (CI) in upwards of 50% of cases,[9] however, the neurobiological substrates of CI in MS remain largely unidentified. Compelling evidence exists that MS-related CI is strongly, and independently, associated with cerebellar pathology,[10] including decreased volume,[11] T1 lesion load (LL),[12] and decreased white matter fractional anisotropy.[13–15] In addition to CI, cerebellar lesion load (CLL) correlates with clinical disability in the setting of ataxia related to MS.[16] Moreover, cerebellar abnormalities prominently contribute to CI in pediatric-onset MS,[17] suggesting the cerebellum serves as an eloquent area in this sub-group.

With this background, and given the new understanding of a motor- cognitive dichotomy in cerebellar functional organization,[1,6] we performed a systematic analysis to explore the relationship between the precise location of lesions within specific cerebellar WM tracts and cognitive status. The purpose of this study was to map the spatial distribution of cerebellar white matter lesions (CWML) across the cerebellar white matter and assess whether this regional distribution differentiates CI and cognitively preserved (CP) MS subjects. By focusing our analysis on the spatially varying probability of CWML, the precise peduncular involvement and association with cognitive status, we sought to expand on previous research that related general cerebellar lesion load and atrophy[11] or, more specifically, total peduncular lesion load[14] to clinical and cognitive disability. Here we show that MS-associated cognitive decline is linked with CWML involving specifically the middle cerebellar peduncles (MCP) but not the superior or inferior cerebellar peduncles. Our results also suggestive of a link between cerebellar lesion patterning and age at symptom onset.

Methods

Subjects

Thirty-one relapsing-remitting MS subjects were recruited from the MGH Multiple Sclerosis Clinic. The study protocol was approved by the Partners Healthcare Human Research Committee IRB at the Massachusetts General Hospital. All subjects provided written informed consent prior to participation. Inclusion criteria: 1) meet McDonald criteria[18] for clinically definite MS; 2) Ages 18–60; 3) Expanded Disability Status Scale (EDSS)[19] of 1.0–6.5 and 4) Able to understand and give informed consent/assent. Disease modifying therapy was allowed. Exclusion criteria: 1) clinical relapse within the previous three months; 2) other structural brain disease; 3) severe depression as measured by the Beck Depression Inventory; 4) other psychiatric disease meeting DSM-IV criteria and 5) severe claustrophobia or MRI contraindication. Twenty-four matched subjects scanned on the same MRI scanner with the same protocols as part of the MGH/USC Human Connectome Project (www.humanconnectomeproject.org) were included as healthy controls (HC). See Table 1 for demographic information for both datasets.

Clinical and Neurocognitive Examination

All patients completed a battery of neuropsychological tests based on the Minimal Assessment of Cognitive Function in MS (MACFIMS)[20] battery. For a given cognitive test, a normalized score two standard deviations or more from established normative values was considered abnormal and patients with at least two abnormal tests were considered cognitively impaired as previously defined.[21,22,23] A neurologist blind to imaging and neuropsychological performance conducted a standard clinical examination, including the EDSS.

Neuroimaging

High-resolution anatomical imaging data were acquired on the 3T Connectom MRI (Siemens AG, Erlangen, Germany) at the Martinos Center for Biomedical Imaging using a 64-channel phased array head coil.[24] Pulse sequence protocols included T1-weighted (T1w) 3D multiecho MPRAGE[25] (TR/TE/TI = 2530/[1.15, 3.03, 4.89, 6.75]/1100 ms, field of view

(FOV) = 256, flip angle (FA) = 7°, GRAPPA acceleration (R) = 2, 1×1×1 mm voxel size), a T2-weighted (T2w) 3D SPACE (TR/TE = 3200/561 ms, FOV = 224, variable FA, R = 2, 0.7×0.7×0.7 mm voxel size) and 3D T2w FLAIR (TR/TE/TI = 5000/389/1800 ms, FOV = 230, R = 2, 7/8 partial Fourier, 0.4×0.4×0.9 mm voxel size) sequences.

Anatomical Image Processing

T1w images were processed through the FreeSurfer automated anatomical pipeline (v. 5.3, http://surfer.nmr.mgh.harvard.edu)[26] to obtain cortical and cerebellar tissue segmentations. An observer blind to cognitive status or disease history manually corrected the resulting segmentations for misclassifications of tissue type (e.g. inferior occipital or temporal cortex classified as proximal cerebellar gray matter). Cortical gray matter volume (CtGMV), cortical white matter volume (CtWMV), cerebellar gray matter volume (CGMV) and cerebellar white matter volume (CWMV) were extracted following manual correction.

Cerebellar and cortical hemispheric white matter lesions were manually segmented on T2w and FLAIR images, respectively, using 3D SLICER (v. 4, www.slicer.com)[27] and separately summed to obtain CLL and hemispheric lesion load (HLL) metrics. Compared to FLAIR images, T2w images are better suited for cerebellar WM lesion segmentation due to a decreased propensity for flow-related artifacts within the cerebellum and better contrast between lesioned tissue and surround normal appearing white matter.[28,29] Cerebellar lesions identified on FLAIR images were substituted in four subjects for whom T2w data were unusable due to low CNR, data corruption or movement artifact. Cerebellar lesion maps were normalized to the SUIT template[30] by first calculating the linear registration between the subject's own T1w image and their T2w image (or FLAIR if substituted for T2w) using FSL (v. 5.0, https://fsl.fmrib.ox.ac.uk/fsl/fslwiki)[31] and then the nonlinear registration between their T1w image and the SUIT cerebellar template using the SUIT toolset. The linear and nonlinear registrations were combined before applying them to the lesion maps with nearest neighbor interpolation. Normalized lesion maps were combined to create a lesion probability map (LPM) summarizing the probability of a lesion occurring in any one voxel of the cerebellum. The Johns Hopkins University cerebellar WM atlas[32] was used to identify the precise location of affected WM within the superior, middle or inferior cerebellar peduncle (SCP, MCP, ICP, respectively) and calculate peduncle-specific lesion load. This probabilistic atlas uses a liberal definition of SCP, MCP and ICP, extending these anatomical fascicles into the corpus of the cerebellar WM based on the fact that fibers traverse those peduncles before entering or leaving cerebellum. However, when discussing our results, we refer to a more strict definition of the MCP described as the massive fasciculus bridging the pons and cerebellum that does not encompass the corpus of the cerebellar white matter.

Voxel Lesion Symptom Mapping Procedure

Voxel-based lesion-symptom mapping (VLSM)[33] was performed using VLSM software (v. 2.55, https://langneurosci.mc.vanderbilt.edu/resources.html). VLSM fits a voxel-wise linear model to the data to investigate the relationship between the presence of a lesion and a regressor of interest, here cognitive status. Age, gender, total cerebellar lesion volume and total cortical lesion volume were included as nuisance covariates in the model. VLSM

t score maps were corrected for multiple comparisons ($p<0.05$) using non-parametric permutation testing (1000 iterations).

Statistical Analysis

Statistical analyses were performed using MATLAB R2016a (The MathWorks, Inc., Natick, MA). Student's t-tests, multiple linear regression, χ^2 tests or Wilcoxon rank sum tests were used as indicated following tests for normality (Tables 1–3). Brain atrophy comparisons included FreeSurfer-derived estimated total intracranial volume (eTIV) as a covariate in linear regression analyses to account for differences in head size. Average brain volumes normalized by eTIV are reported in Table 2. Pearson's correlations were used to test associations between age at symptom onset, disease duration, and lesion load. Kendall's τ was used when testing associations between lesion load and EDSS. Significant tests ($p<0.05$) were Holm-Bonferroni corrected for multiple comparisons.

Results

Clinical Characteristics

The full RRMS group did not differ from the HC group in age or gender ratio, indicating that neither was a factor in group comparisons (Table 1). Among the 31 RRMS subjects, 16 (51.61%) showed evidence of CI as defined in the Methods. The CI and CP groups did not significantly differ on total years of education, EDSS, age at symptom onset or total disease duration, thus removing these as explanatory variables in our group analyses (Table 1).

MRI characteristics

Overall, this RRMS sample did not demonstrate significant cortical or cerebellar atrophy when compared to HC. No significant differences were found for CtGMV, CtWMV, CWMV or CGMV between RRMS and HC or between CP and CI (Table 2). Evidence for CWML was observed in 84% of patients. CP and CI did not significantly differ on any measure of aggregate volumetric lesion load, including cortical, cerebellar or peduncle subdivisions or total lesion load (Table 3). CLL correlated with age at symptom onset ($r=-0.36$, $p<0.05$), but not EDSS ($p=0.69$) or disease duration ($p=0.24$). However, hemispheric lesion load (HLL) was significantly correlated with EDSS ($r=0.40$ $p=0.003$) and not significantly correlated with age at symptom onset ($p=0.87$). The CI and CP specific LPMs revealed visually apparent differences in the spatial distribution of CWML across the cerebellum (Figure 1, Supplemental Videos 1,2,3) for the two groups. The MCP was most likely to be involved (100% of patients with cerebellar lesions), compared to the SCP (58%) and the ICP (84%). Only the CI group exhibited substantial lesion presence across a large portion of the MCP (Figure 1). While there was a relatively large difference in MCP lesion volume between CP and CI (304.8 mm^3), this difference did not reach significance; in part due to the high variability in lesion volume in CI subjects (Table 3). The higher variability for MCP lesion volume is primarily due to a single subject with a relatively higher lesion load than the other CI subjects. Removing this subject reduces the mean and standard deviation to 228.83 and 266.71, respectively, and the lack of a significant group difference remains (Wilcoxon rank-sum, $p = 0.1280$, $z = 1.52$). The CI LPM reveals a higher probability of lesions located in the MCP, rather than in the corpus of the cerebellar white matter (Figure 1).

Cerebellar Voxel Based Lesion Symptom Mapping

VLSM analysis revealed that lesions in bilateral MCP and, to a lesser extent, right ICP were significantly associated with CI (Figure 2, Supplemental Video 4). No significant relationship with cognitive status and either bilateral SCP or left ICP was identified by the VLSM analysis. In concordance with LPMs, the lesions related to CI were located predominantly in the MCP itself and largely spared more posterior areas of the cerebellar white matter.

Discussion

The results of our LPM and VLSM analyses revealed that CI and CP RRMS subjects, despite similar cerebellar lesion volume (Table 2), possess divergent regional distributions of cerebellar lesions. We showed that CI subjects have a higher voxelwise probability of lesions in the MCP, but not the SCP or ICP (Figure 1). VLSM analysis further revealed a significant association between CI and lesions restricted primarily to the MCP proper rather than the corpus of the cerebellar white matter (Figure 2). Finally, we showed that CLL, but not HLL, is related to age at symptom onset and not related to disease duration (Table 2). Importantly, CLL and HLL were not significantly different between groups, suggesting that the distribution of locations of cerebellar white matter lesion, aside from or perhaps in addition to HLL and damage to normal appearing white matter, is an important driving factor of CI in MS. Together, these results suggest that increased presence of lesions within MCP fibers may be related to a younger age at symptom onset and a greater potential for cognitive dysfunction.

The observed relationship between MCP lesions and CI concurs with the relationship hypothesized from the known anatomy of cerebellar connections. Corticocerebellar loops linking cortical motor and association areas reach the cerebellum by way of the pons, and then traverse the MCPs before reaching their destinations in the cerebellar cortex and deep nuclei.[1,2] Lesions of MCP fibers disrupt cerebellar access to motor, cognitive and limbic afferent information from the cerebral cortex. In general, lesions localized to the MCP proper (anterior MCP as defined by the probabilistic atlas) are positioned to disrupt fibers serving an array of cognitive functions; compared to lesions in the corpus of the cerebellar white matter (posterior MCP as defined by the probabilistic atlas), where the fibers would be conveying information of a more specialized nature. In this way, MCP proper lesions should have a large effect on a variety of cognitive functions. Beyond motor ataxia[16], disruption of MCP fiber integrity is therefore expected to impact working memory, reasoning, emotional processing and language skills, all core manifestations of the cerebellar cognitive affective syndrome.[7, 8] MCP lesion load has previously been linked to increased EDSS scores,[14] however our work is the first to reveal the relationship between a specific lesion profile involving the MCP and cognitive decline in MS.

It is worth noting that the CI and CP groups did not differ along several meaningful demographic and atrophy measures, including cerebellar atrophy and lesion load. Cortical and cerebellar atrophy was not demonstrated in the MS group compared to healthy controls. Furthermore, CP and CI samples did not demonstrate significantly different volumes in the cortex or cerebellum, suggesting that our VLSM results are independent of cortical and

cerebellar atrophy. In the future, thalamic and pontine atrophy would be especially relevant to study given their intimate connectivity with the cerebellum. The lack of a significant difference between CP and CI groups in aggregate MCP lesion load is particularly meaningful in light of our VLSM findings; which did find significant cluster of CI- related lesions within the MCP. VLSM is not influenced by variability in lesion load measures and depends solely on colocalization of lesions across subjects and a relationship with the measure of interest. Our VLSM results take advantage of the fact that our subject groups differed primarily in their unique patterns of lesion location.

The relationship between MCP lesions, CI, CLL and age at symptom onset suggests a disease course that may be characterized by early and aggressive disease activity. Our results expand upon research characterizing infratentorial pathology on clinical and cognitive disability in MS,[10–17] providing a detailed account of cerebellar lesion patterning in MS and linking to functional neuroimaging findings of cerebellar topography for cognitive and motor domains. These findings provide motivation for evaluating individual cerebellar lesion profiles in the clinic. In addition, regionally specific cerebellar outcome measures, such as cerebellar lesion profiles, regional (i.e. lobular) cerebellar atrophy and cerebellar functional connectivity, could have additive value in conjunction with other outcomes related to cognition as biomarkers for future clinical trials and interventions targeted to preserve or enhance cognition in MS. This work is limited by the size of the dataset and future work should seek to replicate these findings within a larger, more variable sample. It is well recognized that the exact onset of MS typically pre-dates the first symptom to a variable degree, introducing noise into estimates of age at disease onset. Subsequent research should evaluate these findings in larger, more variable cohorts of RRMS subjects with an evenly distributed age range, ideally with longitudinal data, and also expand these findings into progressive MS subtypes.

Future work could also perform similar analyses within the hemispheric white matter to provide a whole brain assessment of tract-specific contributions to CI in MS. Tract-specific FA reductions within both lesioned and normal appearing hemispheric white matter were related to cognitive impairment and correlates with T2 hyperintense lesion load;[34] suggesting that a tract-specific VLSM approach would also prove fruitful when applied to hemispheric white matter. Such an approach would need to careful consider which tracts to investigate, given the complexity of the cognitive networks in the brain, their structural interconnections and the known profile of CI in MS.[35,36] In addition, research into the differential (and perhaps additive) contribution of specific cerebellar gray and white matter lesion location to cognitive impairment appears promising,[37] but remains to be fully investigated. Our VLSM analysis uncovered a small effect for right hemisphere SCP lesions while the main effect for MCP lesion was bilateral. Future studies could investigate whether a symmetric lesion distribution is an important feature of cerebellum-related CI. Lastly, future work should investigate whether a cerebellar phenotype of MS, possessing specific regional cerebellar involvement and associated clinical indicators, may exist separately from other MS phenotypes.

Conclusion

Cerebellar involvement in MS is a common clinical finding (84% of patients in this study) and summary metrics such as increased lesion count or volume are related to clinical disability and cognitive dysfunction. By analyzing groups with preserved or impaired cognitive ability but balanced lesion loads within the cerebellar white matter and peduncles, our results reveal for the first time that cognitive disability is related to the location of the lesion in the MCP – the massive white matter bundle that conveys associative, paralimbic, and sensorimotor afferents from the cerebral cortex to the cerebellum. This result is a motivating factor for future longitudinal studies of evolving lesion patterns and their relationship with cognitive ability. Individualized assessment of cerebellar lesion location within cerebellar white matter tracts may provide an important biomarker for future cognitive decline in MS.

Supplementary Material

Refer to Web version on PubMed Central for supplementary material.

Acknowledgments

This work was supported by a grant from the National Institutes of Health [K23NS078044–04 (ECK)]. Human Connectome Project data were provided [in part] by the Human Connectome Project, MGH-USC Consortium (Principal Investigators: Bruce R. Rosen, Arthur W. Toga and Van Wedeen; U01MH093765) funded by the NIH Blueprint Initiative for Neuroscience Research grant; the National Institutes of Health grant P41EB015896; and the Instrumentation Grants S10RR023043, 1S10RR023401, 1S10RR019307.

MS Journal Appendix for MRI methodology

Hardware	
Field strength	3-Tesla
Manufacturer	Siemens
Model	Connectom
Coil type (e.g. head, surface)	head
Number of coil channels	64

Acquisition sequence	
Type (e.g. FLAIR, DIR, DTI, fMRI)	T1 MEMPRAGE
Acquisition time	6:02
Orientation	Sagittal
Alignment (e.g. anterior commissure/poster commissure line)	Anterior commissure/posterior commissure line
Voxel size	1 mm isotropic
TR	2530 ms
TE	1.15, 3.03, 4.89, 6.75 ms
Tl	1100 ms

Acquisition sequence		
Flip angle	7 deg	
NEX	1	
Field of view	256	
Matrix size	256 × 256	
Parallel imaging	**Yes**	No
If used, parallel imaging method: (e.g. SENSE, GRAPPA)	GRAPPA = 2	
Cardiac gating	Yes	**No**
If used, cardiac gating method: (e.g. PPU or ECG)		
Contrast enhancement	Yes	**No**
If used, provide name of contrast agent, dose and timing of scan post-contrast administration		
Other parameters:		

Acquisition sequence		
Type (e.g. FLAIR, DIR, DTI, fMRI)	T2 FLAIR	
Acquisition time	5:47	
Orientation	Sagittal	
Alignment (e.g. anterior commissure/poster commissure line)	Anterior commissure/posterior commissure line	
Voxel size	0.4 × 0.4 × 0.9 mm	
TR	5000 ms	
TE	389 ms	
Tl	1800 ms	
Flip angle	variable	
NEX	1	
Field of view	230	
Matrix size	256 × 256	
Parallel imaging	**Yes**	No
If used, parallel imaging method: (e.g. SENSE, GRAPPA)	GRAPPA = 2	
Cardiac gating	Yes	**No**
If used, cardiac gating method: (e.g. PPU or ECG)		
Contrast enhancement	Yes	**No**
If used, provide name of contrast agent, dose and timing of scan post-contrast administration		
Other parameters:		

Acquisition sequence	
Type (e.g. FLAIR, DIR, DTI, fMRI)	T2 SPACE

Acquisition sequence		
Acquisition time	5:57	
Orientation	Sagittal	
Alignment (e.g. anterior commissure/poster commissure line)	Anterior commissure/posterior commissure line	
Voxel size	0.7 mm isotropic	
TR	3200 ms	
TE	561 ms	
Tl	1100 ms	
Flip angle	7 deg	
NEX	1	
Field of view	256	
Matrix size	256 × 256	
Parallel imaging	**Yes**	No
If used, parallel imaging method: (e.g. SENSE, GRAPPA)	GRAPPA = 2	
Cardiac gating	Yes	**No**
If used, cardiac gating method: (e.g. PPU or ECG)		
Contrast enhancement	Yes	**No**
If used, provide name of contrast agent, dose and timing of scan post-contrast administration		
Other parameters:		

Image analysis methods and outputs	
Lesions	
Type (e.g. Gd-enhancing, T2-hyperintense, T1-hypointense)	T2-hyperintense
Analysis method	Hand segmentation
Analysis software	3D Slicer (www.slicer.org)
Output measure (e.g. count or volume [ml])	Volume [mm^3]
Tissue volumes	
Type (e.g. whole brain, grey matter, white matter, spinal cord)	Cortical gray and white matter, cerebellar gray and white matter
Analysis method	Automated segmentation with manual correction
Analysis software	FreeSurfer v. 5.3 (https://surfer.nmr.mgh.harvard.edu)
Output measure (e.g. absolute tissue volume in ml, tissue volume as a fraction of intracranial volume, percentage change in tissue volumes)	Absolute tissue volume [mm^5] for group comparison and analysis, absolute tissue volume normalized by intracranial volume for reporting group averages
Tissue measures (e.g. MTR, DTI, T1-RT, T2-RT, T2*, T2', ^{1}H-MRS, perfusion, Na)	
Type (e.g. whole brain, grey matter, white matter, spinal cord, normal-appearing grey matter or white matter)	
Analysis method	
Analysis software	
Output measure	

Image analysis methods and outputs	
Other MRI measures (e.g. functional MRI)	
Type (e.g. whole brain, grey matter, white matter, spinal cord, normal-appearing grey matter or white matter)	
Analysis method	
Analysis software	
Output measure	

Other analysis details:

References

1. Schmahmann JD. The role of the cerebellum in cognition and emotion: Personal reflections since 1982 on the dysmetria of thought hypothesis, and its historical evolution from theory to therapy. Neuropsychol Rev 2010; 20(3):236–60. [PubMed: 20821056]
2. Schmahmann JD, Pandya DN. The cerebrocerebellar system. In: Schmahmann JD, ed. The Cerebellum and Cognition. San Diego, Academic Press. Int Rev Neurobiol 1997; 41:31–60.
3. Strick PL, Dum RP, Fiez JA. Cerebellum and nonmotor function. Annu Rev Neurosci 2009; 32:413–34. [PubMed: 19555291]
4. Buckner RL, Krienen FM, Castellanos A, et al. The organization of the human cerebellum estimated by intrinsic fuctional connectivity. J Neurophysiol 2011; 106(5):2322–45. [PubMed: 21795627]
5. Desmond JE, Gabrieli JD, Wagner AD et al. Lobular patterns of cerebellar activation in verbal working-memory and finger-tapping tasks as revealed by functional MRI. J Neurosci 1997; 17(24):9675–85. [PubMed: 9391022]
6. Stoodley CJ, Valera EM, Schmahmann JD. Functional topography of the cerebellum for motor and cognitive tasks: an fMRI stud. Neuroimage 2012; 59(2):1560–70. [PubMed: 21907811]
7. Schmahmann JD and Sherman JC. The cerebellar cognitive affective syndrome. Brain 1998; 121:561–579. [PubMed: 9577385]
8. Schmahmann JD. Disorders of the cerebellum: ataxia, dysmetria of thought, and the cerebellar cognitive affective syndrome. J Neuropsychiatry Clin Neurosci 2004; 16:367–78. [PubMed: 15377747]
9. Amato MP, Portaccio E, Goretti B, et al. Cognitive impairment in early stages of multiple sclerosis. Neurol Sci 2010; 31:S211–214. [PubMed: 20640466]
10. Weier K, Banwell B, Cerasa A, et al. The role of the cerebellum in multiple sclerosis. Cerebellum 2015; 14:364–74. [PubMed: 25578034]
11. Weier K, Penner IK, Magon S, et al. Cerebellar abnormalities contribute to disability including cognitive impairment in multiple sclerosis. PLoS ONE 2014; 9(1):e86916. [PubMed: 24466290]
12. Valentino P, Cerasa A, Chiriaco C, et al. Cognitive deficits in multiple sclerosis patients with cerebellar symptoms. Mult Scler 2009; 15(7):854–9. [PubMed: 19542264]
13. Deppe M, Tabelow K, Kramer J, et al. Evidence for early, non-lesional cerebellar damage in patients with multiple sclerosis: DTI measures correlate with disability, atrophy, and disease duration. Mult Scler 2016; 22(1):73–84. [PubMed: 25921041]
14. Preziosa P, Rocca MA, Mesaros S, et al. Relationship between damage to the cerebellar peduncles and clinical disability in multiple sclerosis. Radiology 2014; 271(3):822–830. [PubMed: 24555637]
15. Sbardella E, Petsas N, Tona F, et al. Assessing the correlation between grey and white matter damage with motor and cognitive impairment in multiple sclerosis patients. PloS ONE 2013; 8(5):e63250. [PubMed: 23696802]
16. Hickman SJ, Brierley CM, Silver NC, et al. Infratentorial hypointense lesion volume on T1-weighted magnetic resonance imaging correlates with disability in patients with chronic cerebellar ataxia due to multiple sclerosis. J Neurol Sci 2001; 187(1–2):35–9. [PubMed: 11440742]

17. Weier K, Till C, Fonov V, et al. Contribution of the cerebellum to cognitive performance in children and adolescents with multiple sclerosis. Mult Scler 2016; 22(5):599–607. [PubMed: 26203072]
18. Polman CH, Reingold SC, Edan G, et al. Diagnostic criteria for multiple sclerosis: 2005 revisions to the 'McDonald Criteria'. Ann Neurol 2005; 58(6):840–6. [PubMed: 16283615]
19. Kurtzke JF. Rating neurologic impairment in multiple sclerosis: an expanded disability status scale (EDSS). Neurology 1983; 33(11):1444–52 [PubMed: 6685237]
20. Benedict RHB, Cookfair D, Gavett R, et al. Validity of the Minimal Assessment of Cognitive Function in Multiple Sclerosis (MACFIMS). J Int Neuropsychol Soc 2006; 11:574–558.
21. Feinstein A, Lapshin H, O'Connor P. Looking anew at cognitive dysfunction in multiple sclerosis: the gorilla in the room. Neurology 2012; 79(1):1124–9 [PubMed: 22933746]
22. Patel VP, Walker LA, Feinstein A. Revisiting cognitive reserve and cognition in multiple sclerosis: A closer look at depression. Mult Scler 2017: 1352348517692887.
23. Patel V, Zambrana A, Walker L, et al. Distraction adds to the cognitive burden in multiple sclerosis. Mult Scler 2016: 135245851664120.
24. Keil B, Blau Jn, Biber S, et al. A 64-channel 3T array coil for acceleraed brain MRI. Magn Reson Med 2013; 7091:248–58.
25. van der Kouwe AJJ, Benner T, Salat DH, Fischl B. Brain morphometry with multiecho MPRAGE. Neuroimage 2008; 40(2):559–69. [PubMed: 18242102]
26. Fischl B FreeSurfer. Neuroimage 2012; 62(2):774–81. [PubMed: 22248573]
27. Fedorov A, Beichel R, Kalpath-Cramer J, et al. 3D Slicer as an Image Computing Platform for the Quantitative Imaging Network. Magn Reson Imaging 2012; 30(9):1323–41. [PubMed: 22770690]
28. Bailey WM. Fast fluid attenuated inversion recovery (FLAIR) imaging and associated artefacts in magnetic resonance imaging (MRI). Radiography 2007; 13(4):283–90.
29. Klawiter EC. Current and new directions in MRI in multiple sclerosis. Continuum (Minneap Minn). 2013; 19(4 Multiple Sclerosis):1058–73. [PubMed: 23917101]
30. Diedrichsen J A spatially unbiased atlas template of the human cerebellum. Neuroimage 2006; 33(1):127–38. [PubMed: 16904911]
31. Jenkinson M, Beckmann CF, Behrens TE, et al. FSL. NeuroImage 2012; 62:782–90. [PubMed: 21979382]
32. Wakana S, Jiang H, Nagae-Poetscher LM, et al. Fiber tract-based atlas of human white matter anatomy. Radiology 2004; 230(1):77–87. [PubMed: 14645885]
33. Bates E, Wilson SM, Saygin AP, et al. Voxel-based lesion-symptom mapping. Nat Neurosci 2003; 6(5):448–50. [PubMed: 12704393]
34. Yu HJ, Christodoulou C, Bhise V, et al. Multiple white matter tract abnormalities underlie cognitive impairment in RRMS. Neuroimage. 2012; 59(4):3713–22. [PubMed: 22062194]
35. Winkelmann C, Engel C, Apel A, Zetti UK. 2007. Cognitive impairment in multiple sclerosis. J Neurol 254 (Suppl 2):1135–1142. [PubMed: 17294066]
36. Chiaravalloti ND, DeLuca J. 2008. Cognitive impairment in MS. Lancet Neurol 7:1139–1151. [PubMed: 19007738]
37. Damasceno A, Damasceno BP, Cendes F. The clinical impact of cerebellar grey matter pathology in multiple sclerosis PLoS ONE 2014; 9(5):e9619

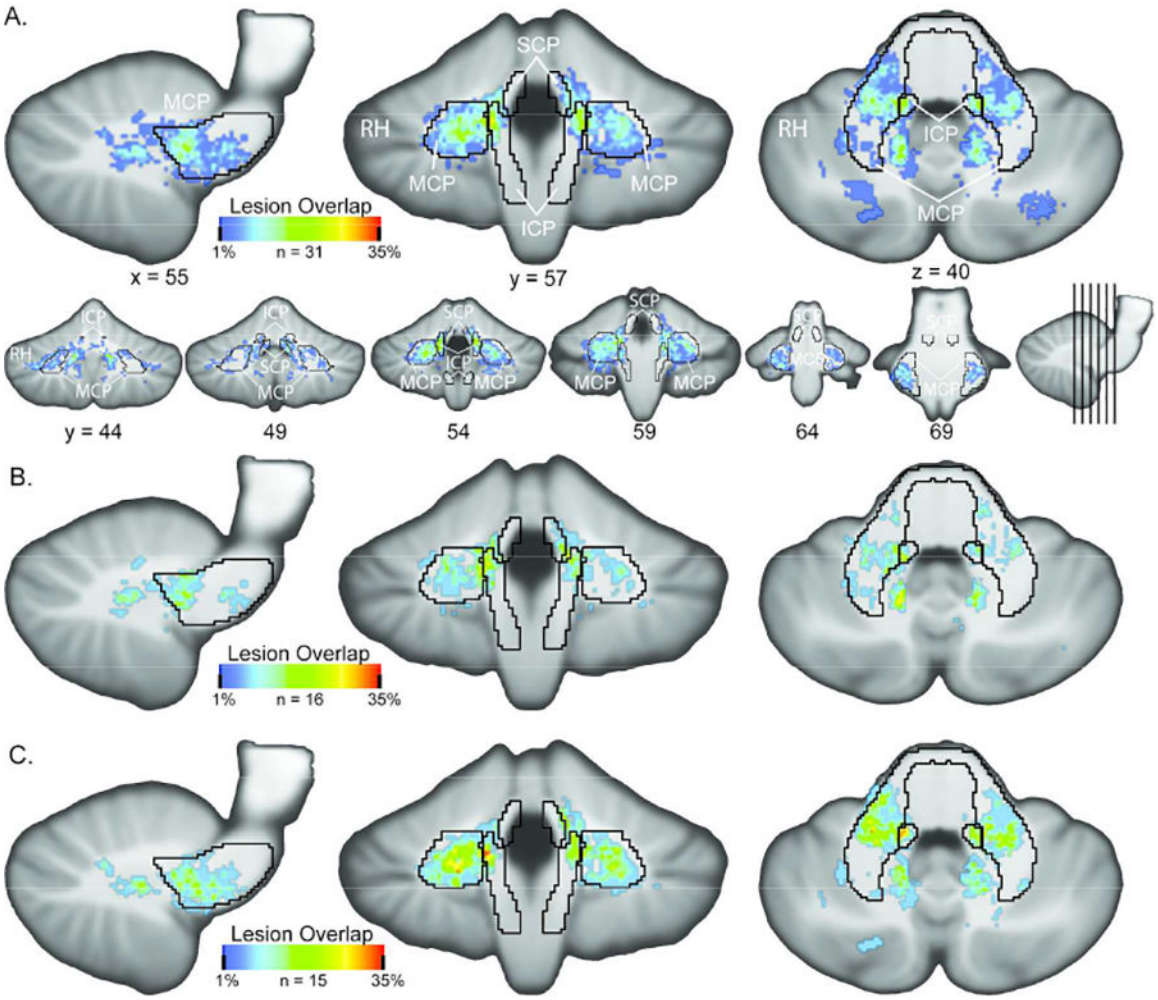

Figure 1:

Lesion Probability Mapping Results Lesion probability maps for (A) entire RRMS, (B) cognitive preserved and (C) cognitive impaired samples. RRMS demonstrated a strong predilection for MCP lesions (100% of patients with cerebellar lesions), a lower probability of ICP lesion (84%) and significantly lower probability of SCP lesion (58%) The spatial spread of increased probability of MCP lesions in CI over CP is clearly visible in panels B and C. See Supplemental Movies 1,2 and 3 for coronal slice-by-slice roll throughs of the LPM data for the entire RRMS, CI and CP MS groups, respectively. Area borders correspond to the John's Hopkins University white matter atlas mapped to SUIT template space. SCP = superior cerebellar peduncle; MCP = middle cerebellar peduncle; ICP = inferior cerebellar peduncle.

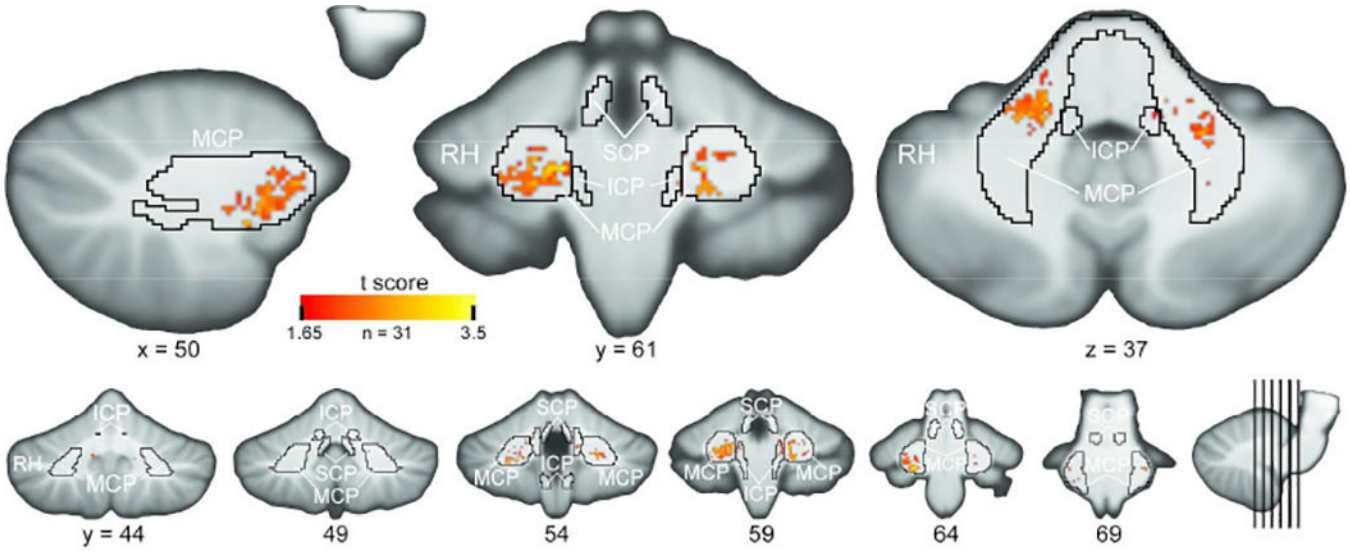

Figure 2:

Voxel-Lesion Symptom Mapping Analysis Results. The t-statistic map from the VLSM regression analysis of the relationship between cognitive status and lesion location is displayed. Cerebellar regions associated with increased cognitive impairment are nearly completely restricted to the MCP. Map is threshold at $p < 0.05$ corrected for multiple comparisons via permutation testing (1000 iterations). See Supplemental Movie 4 for a coronal slice-by-slice roll through of the VLSM data. Area borders correspond to the Johns Hopkins University white matter atlas mapped to SUIT template space. SCP = superior cerebellar peduncle; MCP = middle cerebellar peduncle; ICP = inferior cerebellar peduncle.

Table 1:

Demographic Information and Group Comparisons.

				MS vs. HC[a]		CP vs. CI	
	CP (n=15)	CI (n=16)	HC (n=24)	Test Stat.	*p* Value	Test Stat.	*p* Value
Age, mean (SD)	41.19 (2.47)	41.33 (3.17)	36.46 (10.67)	1.63	0.11[b]	0.04	0.97[b]
Gender, M:F	4:11	5:11	13:11	3.56	0.06[c]	0.08	0.78[c]
Education, mean (SD)	16.19	15.93	N/A			−0.34	0.74[b]
EDSS, median (range)	2 (1–4)	2 (1–6.5)	N/A			0.19	085[d]
Age at Disease Onset, mean (SD)	34.5 (8.59)	32.27 (10.51)	N/A			−0.65	0.52[b]
Disease Duration, mean (SD)	6.69 (5.99)	9.07 (6.49)	N/A			1.06	0.30[b]

Abbreviations: CP = Cognitively Preserved; CI = Cognitively Impaired; HC = Healthy Control; EDSS = Expand Disability Status Scale.

[a] MS versus HC group comparisons conducted with entire MS sample.

[b] Student's t-test.

[c] χ^2 test.

[d] Wilcoxon rank sum test.

Table 2:

Atrophy measurements and group comparisons.

				MS vs. HC[a]		CP vs. CI	
	CP (n=15)	**CI (n=16)**	**HC (n=24)**	**Test Stat.**	***p* Value**	**Test Stat.**	***p* Value**
CtGMV, mean (sd)	0.300 (0.021)	0.276 (0.025)	0.288 (0.021)	1.24	0.30[b]	2.11	0.14[b]
CtWMV, mean (SD)	0.286 (0.020)	0.297 (0.021)	0.300 (0.018)	1.28	0.29[b]	1.46	0.25[b]
CGMV, mean (SD)	0.064 (0.005)	0.062 (0.007)	0.064 (0.007)	−1.09	0.28[b]	−1.44	0.16[b]
CWMV, mean (SD)	0.017 (0.003)	0.019 (0.003)	0.018 (0.002)	−0.17	0.87[b]	1.08	0.29[b]

All volumetric measurements are reported in mm^3 and were normalized for head size. Un-normalized volumetric measurements were used in conjunction with a covariate for head size in linear regression analyses. Abbreviations: CP = Cognitively Preserved; CI = Cognitively Impaired; HC = Healthy Control; CtGMV – Cortical Gray Matter Volume; CtWMV = Cortical White Matter Volume; CGMV = Cerebellar Gray Matter Volume; CWMV = Cerebellar White Matter Volume.

[a] MS versus HC group comparisons conducted with entire MS sample.

[b] Multiple linear regression.

Table 3:

Lesion Load Characteristics and Group Comparisons.

	CP (n=15)	CI (n=16)	Test Stat.	*p* Value
HLL, mean (SD)	3801.8 (2324.7)	8254.7 (8599.9)	2.00	0.06[b]
TCLL, mean (SD)	408.62 (284.10)	548.38 (498.49)	0.97	0.34[b]
SCP, mean (SD)	25.63 (38.49)	18.67 (35.41)	−0.39	0.70[c]
MCP, mean (SD)	167.00 (202.77)	471.80 (824.33)	1.52	0.13[c]
ICP, mean (SE SD	57.63 (63.09)	62.73 (70.47)	0.14	0.89[c]

All volumetric measures reported in mm^3. Abbreviations: CP = Cognitively Preserved; CI = Cognitively Impaired; HC = Healthy Control; HLL = Hemispheric Lesion Load; TCLL = Total Cerebellar Lesion Load; SCP = Superior Cerebellar Peduncle; MCP = Middle Cerebellar Peduncle; ICP = Inferior Cerebellar Peduncle.

[a] MS versus HC group comparisons conducted with entire MS sample.

[b] Student's t-test. test.

[c] Wilcoxon rank sum test.